



Cite this: *Dalton Trans.*, 20xx, 00, 0000

# Exploiting 1,4-naphthoquinone and 3-iodo-1,4-naphthoquinone motifs as anion binding sites by hydrogen or halogen-bonding interactions † ‡

Encarnación Navarro-García,<sup>a</sup> María D. Velasco,<sup>a</sup> Fabiola Zapata,<sup>a</sup> Antonio Bauzá,<sup>b</sup> Antonio Frontera,<sup>b</sup> Carmen Ramírez de Arellano<sup>c</sup> and Antonio Caballero\*<sup>a</sup>

We describe here the utilization of 1,4-naphthoquinone and 3-iodo-1,4-naphthoquinone motifs as new anion binding sites by hydrogen- or halogen-bonding interactions, respectively. These binding sites have been integrated in bidentate ester based receptors. Emission experiments reveal that both receptors selectively recognize sulfate anions, which induced a remarkable increase of a new emission band attributed to the formation of  $\pi$ -stacking interactions between two 1,4-naphthoquinone units. Absorption spectroscopy and mass spectrometry indicate the disruption of the ester group of the 1,4-naphthoquinone based receptor in the presence of  $\text{HP}_2\text{O}_7^{3-}$ ,  $\text{H}_2\text{PO}_4^-$ ,  $\text{F}^-$ ,  $\text{AcO}^-$  and  $\text{C}_6\text{H}_5\text{CO}_2^-$  and in the halogenated receptor with  $\text{HP}_2\text{O}_7^{3-}$ ,  $\text{F}^-$  and  $\text{AcO}^-$  anions, while the presence of sulfate anions showed the classical complexation behaviour. The  $^1\text{H-NMR}$  experiment showed a slow exchange process of the receptors with their sulfate complexes. The binding mode of the receptors with sulfate has been studied by DFT calculations along with the Molecular Electrostatic Potential (MEP) surface computational tool that reveals those parts of the receptors which are more suitable for interacting with anions.

## Introduction

The development of new molecular receptors capable of recognizing and sensing anionic species is one of the most active areas within supramolecular chemistry. The important role that anions play in numerous chemical, biological and environmental processes justifies the effort of numerous research groups to realize more selective anion receptors.<sup>1</sup>

Since the first use of positively charged ammonium groups for the recognition of anions,<sup>2</sup> they have been described as important motifs of anion binding sites. The hydrogen bond

has been the most popular noncovalent interaction used for this purpose. A majority of hydrogen bonding anion receptors employ N–H functionalities as hydrogen bond donors. Despite the presence of the CVO hydrogen bond acceptor, amides<sup>3</sup> and ureas<sup>4</sup> have been extensively used as anion binding sites by hydrogen bond interactions. Other anion binding sites which use the N–H group are the pyrrole and indole groups.<sup>5</sup> Interestingly, in recent years, C–H hydrogen bond donors have also become popular. Specifically, hydrogen at position 5 of the 1,2,3-triazole ring has been successfully used as a binding site in the design of new anion receptors.<sup>6</sup> On the other hand, the alkylation of the N-3 of the 1,2,3-triazole ring conduces to an anion binding site which combines the strength of the electrostatic interaction and the relative directionality of the hydrogen-bonding interaction.<sup>7</sup> In the same sense, the imidazolium cation uses the H-2 of the imidazolium ring as the anion binding site.<sup>8</sup>

More recently, the halogen bond has proven to be an excellent alternative to the hydrogen bond in the design of novel anion binding sites.<sup>9</sup> Halogen bond is a noncovalent interaction between halogen atoms with electrophilic centres (Lewis acids) and neutral or anionic Lewis bases.<sup>10</sup> The origin of this non covalent interaction is explained based on the anisotropy of the electrostatic potential in the halogen atom where the positive charge is located at the terminus of the R–X

<sup>a</sup>Departamento de Química Orgánica, Universidad de Murcia, Campus de Espinardo, 30100 Murcia, Spain. E-mail: antocaba@um.es

<sup>b</sup>Departament de Química, Universitat de les Illes Balears, Crta. de Valldemossa Km75, 07122 Palma de Mallorca, Balears, Spain

<sup>c</sup>Departamento de Química Orgánica, Universidad de Valencia, E-46100 Valencia, Spain

† Dedicated to the memory of Professor Molina, a great source of inspiration in our work.

‡ Electronic supplementary information (ESI) available:  $^1\text{H}$  and  $^{13}\text{C}$  NMR spectra, fluorescence anion binding studies, Job plot experiments,  $^1\text{H}$  NMR experiments, computational details and Cartesian coordinates, NMR spectra, fluorescence and  $^1\text{H-NMR}$  anion binding studies and computational results. CCDC 1915911. For ESI and crystallographic data in CIF or other electronic format see DOI: 10.1039/c9dt02012h

axis ( $\sigma$  hole), while a band of negative charge remains around the equator.<sup>11</sup> To date, practically all the anion receptors based on halogen bond interaction described in the literature use the 1,2,3-halotriazolium,<sup>12</sup> haloimidazolium<sup>13</sup> or halopyridinium<sup>14</sup> rings as charge assisted anion binding sites or much more rarely the haloperfluorobenzene<sup>15</sup> or 1,2,3-halotriazole<sup>16</sup> rings as neutral anion binding sites.

Surprisingly, to the best of our knowledge, and despite the well-known electron-deficient characteristic of the 1,4-naphthoquinone unit, which makes it an excellent candidate to act as the anion binding site, its ability as an anion binding site has not been reported to date. Even more, taking into account that the anthraquinone, 1,4-naphthoquinone, and benzoquinone motifs have been used as cation binding sites and as colorimetric and fluorescence signalling units in several anion and cation receptors.<sup>17</sup>

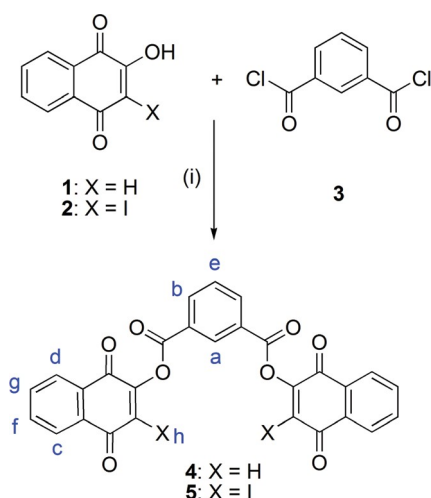
With the aim of providing new anion binding sites for the design of novel anion receptors, we describe herein the utilization of 1,4-naphthoquinone and 3-iodo-1,4-naphthoquinone as hydrogen- or halogen-binding sites for anions, respectively, integrated in two novel neutral bidentate ester based receptors.

## Results and discussion

### Synthesis

The ester based receptors 4 and 5 were obtained by treating the commercially available 2-hydroxy-1,4-naphthoquinone 1 or the previously described 2-hydroxy-3-iodo-1,4-naphthoquinone 2<sup>18</sup> with isophthaloyl dichloride 3 in the presence of 2,6-lutidine as a base in  $\text{CH}_2\text{Cl}_2$  at 0 °C (Scheme 1).

Receptors 4 and 5 were obtained in good yields of 84 and 67%, respectively, and were fully characterized using standard techniques: <sup>1</sup>H NMR, <sup>13</sup>C NMR and FAB mass spectrometry.



Scheme 1 Synthesis of the ester based receptors bis(1,4-naphthoquinone-2-yl) isophthalate 4 and bis(3-iodo-1,4-naphthoquinone-2-yl) isophthalate 5. Reagents and conditions: (i) 2,6-Lutidine,  $\text{CH}_2\text{Cl}_2$ , 0 °C, 20 min, yield 84–67%.

### Anion binding studies

The anion-recognition properties of bis 1,4-naphthoquinone receptors 4 and 5 were evaluated by UV-Vis, fluorescence and <sup>1</sup>H NMR spectroscopy of several anions:  $\text{HP O}_4^{3-}$ ,  $\text{H PO}_4^{2-}$ ,  $\text{HSO}_4^-$ ,  $\text{NO}_3^-$ ,  $\text{F}^-$ ,  $\text{Cl}^-$ ,  $\text{Br}^-$ ,  $\text{I}^-$ ,  $\text{AcO}^-$ ,  $\text{ClO}_4^-$ ,  $\text{BF}_4^-$ ,  $\text{PF}_6^-$  and  $\text{C}_6\text{H}_5\text{CO}_2^-$  as tetrabutylammonium salts and  $\text{SO}_4^{2-}$  as tetramethylammonium salts.

The UV-Vis spectra of the receptors 4 and 5 in  $\text{CH}_3\text{CN}$  present two intense absorption bands at  $\lambda = 245$  ( $\epsilon = 58\,570\text{ M}^{-1}\text{ cm}^{-1}$ ) and 250 nm ( $\epsilon = 58\,995\text{ M}^{-1}\text{ cm}^{-1}$ ) for receptor 4 and  $\lambda = 245$  ( $\epsilon = 72\,884\text{ M}^{-1}\text{ cm}^{-1}$ ) and 252 nm ( $\epsilon = 34\,858\text{ M}^{-1}\text{ cm}^{-1}$ ) for the halogenated receptor 5. In addition to these bands, another weaker absorption band is present at  $\lambda = 336$  nm in both receptors.

The addition of increasing amounts of  $\text{HP}_2\text{O}_7^{3-}$ ,  $\text{H}_2\text{PO}_4^-$ ,  $\text{F}^-$ ,  $\text{AcO}^-$  and  $\text{C}_6\text{H}_5\text{CO}_2^-$  to a solution of receptor 4 ( $c = 5 \times 10^{-5}\text{ M}$  in  $\text{CH}_3\text{CN}$ ) or  $\text{HP}_2\text{O}_7^{3-}$ ,  $\text{F}^-$  and  $\text{AcO}^-$  to a solution of the halogenated receptor 5 ( $c = 5 \times 10^{-5}\text{ M}$  in  $\text{CH}_3\text{CN}$ ), induces important perturbations in the absorption spectra of the receptors. These changes consisted in the progressive grown of a weak and broad absorption band in the visible region centered at  $\lambda = 478$  nm for receptor 4 and  $\lambda = 488$  nm for the halogenated receptor 5 during the addition of increasing amounts of the previously mentioned anions and it is the cause for the dramatic change of color of the dissolution of receptors 4 and 5 from colorless to orange (Fig. 1a). After proving the dependence of the  $\lambda_{\text{max}}$  of this new band on the solvent used, this new band is assigned to a charge transfer process. Thus, a shift of the  $\lambda_{\text{max}}$  to a shorter wavelength was observed for receptor 4 in  $\text{CH}_3\text{NO}_2$  ( $\lambda = 468$  nm) as compared to THF

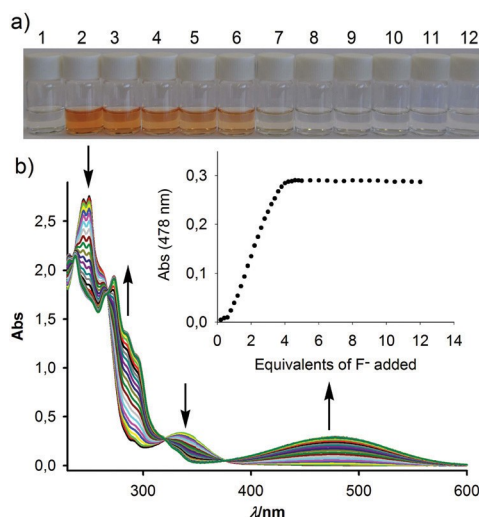


Fig. 1 (a) Changes in the colour of a solution of receptor 4 (1) in  $\text{CH}_3\text{CN}$  upon the addition of  $\text{F}^-$  (2),  $\text{AcO}^-$  (3),  $\text{HP}_2\text{O}_7^{3-}$  (4),  $\text{C}_6\text{H}_5\text{CO}_2^-$  (5),  $\text{H}_2\text{PO}_4^-$  (6),  $\text{SO}_4^{2-}$  (7),  $\text{HSO}_4^-$  (8),  $\text{NO}_3^-$  (9),  $\text{Cl}^-$  (10),  $\text{Br}^-$  (11) and  $\text{I}^-$  (12). (b) Changes in the absorption spectra of receptor 4 ( $c = 5 \times 10^{-5}\text{ M}$  in  $\text{CH}_3\text{CN}$ ) upon the addition of increasing amounts of  $\text{F}^-$  anions. The arrows indicate the absorption that increases or decreases during the titration. Inset: Changes in the absorption of receptor 4 upon increasing addition of  $\text{F}^-$  anions monitored at  $\lambda = 478$  nm.

( $\lambda = 488$  nm); while  $\lambda_{\max}$  appears at  $\lambda = 478$  nm and  $\lambda = 480$  nm in  $\text{CH}_3\text{CN}$  and  $\text{CH}_2\text{Cl}_2$ , respectively, a similar behaviour was also observed in the halogenated receptor 5 (see the ESI Fig. S20 and S21†). The negative solvatochromism observed with more polar solvents is characteristic of the CT bands. The band centered at  $\lambda = 336$  nm disappears during the titration (Fig. 1b and S9–S18†).

Additionally, the modification of the absorption bands is not only dependent on the number of equivalents of anions added but also depends on the time, which suggests that a chemical modification is taking place in the receptors in the presence of those anions. Taking this into account, the anion addition processes were monitored by mass spectrometry. These experiments clearly indicated that the presence of  $\text{HP}_2\text{O}_7^{3-}$ ,  $\text{H}_2\text{PO}_4^-$ ,  $\text{F}^-$ ,  $\text{AcO}^-$  and  $\text{C}_6\text{H}_5\text{CO}_2^-$  in a solution of receptor 4 or  $\text{HP}_2\text{O}_7^{3-}$ ,  $\text{F}^-$  and  $\text{AcO}^-$  in a solution of the halogenated receptor 5 in  $\text{CH}_3\text{CN}$  causes the disruption of the ester group into the corresponding 3-X-1,4-dioxo-1,4-dihydronaphthalen-2-olate ( $X = \text{H}, \text{I}$ ) and 3-carboxybenzoate (see the ESI Fig. S24–S29†). The CT band is assigned to an intramolecular charge transfer from the deprotonated hydroxyl group to the 1,4-naphthoquinone ring. This assignment was supported by UV-Vis experiments on the 2-hydroxy-1,4-naphthoquinone where the addition of  $\text{OH}^-$  promotes the appearance of identical CT bands (see the ESI Fig. S14 and S18†).

The disruption of the ester group caused by  $\text{AcO}^-$  anions was also confirmed by X-ray diffraction experiments on several

crystals obtained by vapor diffusion of diethyl ether into a solution of both the halogenated receptor 5 and  $\text{AcO}^-$  in  $\text{CH}_3\text{CN}$ . In the X-ray experiments, two different types of crystals with two different unit cells were found. For the first type of crystal, the structure of the tetrabutyl ammonium salt of 3-iodo-1,4-dioxo-1,4-dihydronaphthalen-2-olate was solved (Fig. 2). Although, different polymorphs for the structure of 3-iodolawsone have been reported, we have not found any structure containing the anion 1,4-dioxo-1,4-dihydronaphthalen-2-olate in the CSD database.<sup>19</sup> O–H $\cdots$ O and  $\pi\cdots\pi$  stacking

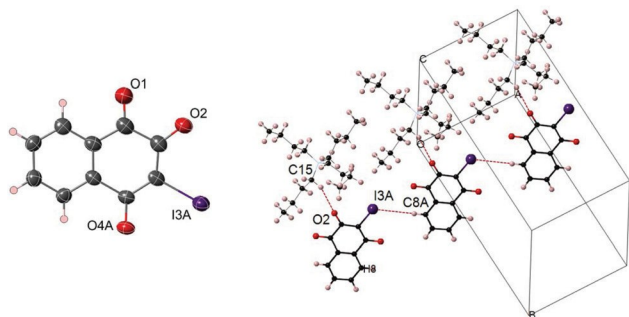


Fig. 2 X-ray thermal ellipsoid plot for the anion of 3-iodo-1,4-dioxo-1,4-dihydronaphthalen-2-olate (50% probability level) (left) and crystal packing view showing the shortest anion $\cdots$ cation and anion $\cdots$ anion interactions (right). The main component of the disordered moiety is shown.

arrangements are common features reported for the different polymorphs of neutral 3-iodolawsone. In the reported structure, the shortest interactions are anion $\cdots$ cation C–H $\cdots$ O bonds [C15–H15B $\cdots$ O2: C15  $\cdots$ O2 3.286(6) Å, H15B $\cdots$ O2 2.43 Å, C15–H15B $\cdots$ O2 144.4°]. Furthermore, C–H $\cdots$ I contacts [C8A–H8A $\cdots$ I3A<sup>i</sup> (i:  $x - 1, y, z$ ): C8A $\cdots$ I3A 4.213(14) Å, H8A $\cdots$ I3A 3.27 Å, C8A–H8A $\cdots$ I3A 169.6°] are the shortest anion $\cdots$ anion contacts found in the structure (Fig. 2). For the second type of crystal, the unit cell and preliminary data confirmed the presence of the tetrabutyl ammonium salt of 3-carboxybenzoate (see ESI part VII†). A water solvate of tetrabutyl ammonium 3-carboxybenzoate has been reported.<sup>20</sup>

On the other hand, the addition of increasing amounts of  $\text{SO}_4^{2-}$  anions to a solution of receptors 4 and 5 ( $c = 5 \times 10^{-5}$  M in  $\text{CH}_3\text{CN}$ ) induced different perturbations in their absorption spectra with regards to the behavior observed in receptor 4 with  $\text{HP}_2\text{O}_7^{3-}$ ,  $\text{H}_2\text{PO}_4^-$ ,  $\text{F}^-$ ,  $\text{AcO}^-$  and  $\text{C}_6\text{H}_5\text{CO}_2^-$  and in the halogenated receptor 5 with  $\text{HP}_2\text{O}_7^{3-}$ ,  $\text{F}^-$  and  $\text{AcO}^-$  anions. In this case, the presence of  $\text{SO}_4^{2-}$  anions promotes the increase of the intensity and a red shift in the absorption band at  $\lambda = 336$  nm of  $\Delta\lambda = 7$  nm for receptor 4 and  $\Delta\lambda = 23$  nm for receptor 5, and these changes are consistent with a complexation process. Nevertheless, the presence of  $\text{SO}_4^{2-}$  anions also promotes the apparition of a very weak CT band at  $\lambda = 465$  nm in receptor 4 (see the ESI Fig. S13†) indicating that  $\text{SO}_4^{2-}$  anions are able to disrupt the ester groups although in a small portion. Interestingly, this CT band is completely absent during the addition of the  $\text{SO}_4^{2-}$  anion to the halogenated receptor 5 (Fig. 3a).

The presence of several isosbestic points was detected during the titration. The stoichiometry of the complexes was determined by Job's plot experiment and the results reveal a 2 : 1 receptor to anion stoichiometry in both receptors for  $\text{SO}_4^{2-}$  anions (Fig. 3b).

The addition of  $\text{HSO}_4^-$ ,  $\text{NO}_3^-$ ,  $\text{Cl}^-$ ,  $\text{Br}^-$ ,  $\text{I}^-$ ,  $\text{ClO}_4^-$ ,  $\text{BF}_4^-$  and  $\text{PF}_6^-$  had no effect on the absorption spectra of the receptors 4

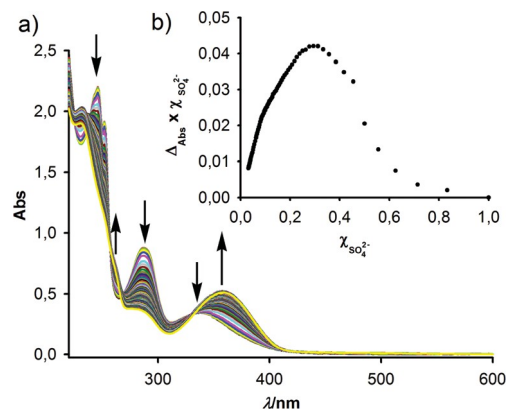


Fig. 3 (a) Changes in the absorption spectra of receptor 5 ( $c = 5 \times 10^{-5}$  M in  $\text{CH}_3\text{CN}$ ) upon the addition of increasing amounts of  $\text{SO}_4^{2-}$  anions. The arrows indicate the absorption that increases or decreases during the titration. (b) Job plot experiment with the maximum at 0.33 indicating a 2 : 1 stoichiometry of receptor 5 to  $\text{SO}_4^{2-}$  anions.

Table 1 Calculated association constants for receptors 4 and 5 with  $\text{SO}_4^{2-}$  anions in  $\text{CH}_3\text{CN}$  by absorption spectroscopy. The errors (in percent) are given in parenthesis

4	5
$K_1 = 1.0 \times 10^3$ (2)	$K_1 = 1.6 \times 10^3$ (3)
$K_2 = 55$ (1)	$K_2 = 6.3 \times 10^3$ (1)

and 5 even in the presence of a large excess of anions added. Importantly, the presence of  $\text{H}_2\text{PO}_4^-$  and  $\text{C}_6\text{H}_5\text{CO}_2^-$  does not induce any perturbation in the absorption spectrum of the halogenated receptor 5.

The association constant values were calculated by fitting the UV-Vis titration data to the obtained host-guest binding model using the Dynafit program<sup>21</sup> and are collected in Table 1. The results indicate the superior ability of the halogen bonding receptor 5 towards the analogous hydrogen bonding one to bind  $\text{SO}_4^{2-}$  anions. The larger  $K_2$  value observed for receptor 5 can be attributed to additional host-host interactions as detailed in the ESI (see the ESI Fig. S40†).

The ester based receptors 4 and 5 exhibit a very weak fluorescence with rather low quantum yields  $\Phi_4 = 4.773 \times 10^{-5}$  and  $\Phi_5 = 1.7 \times 10^{-5}$  in  $\text{CH}_3\text{CN}$  ( $c = 5 \times 10^{-5}$  M) when excited at  $\lambda_{\text{exc}} = 360$  nm. Upon addition of the above-mentioned set of anions, no changes in their emission spectra were observed for  $\text{HP}_2\text{O}_7^{3-}$ ,  $\text{H}_2\text{PO}_4^-$ ,  $\text{HSO}_4^-$ ,  $\text{NO}_3^-$ ,  $\text{F}^-$ ,  $\text{Cl}^-$ ,  $\text{Br}^-$ ,  $\text{I}^-$ ,  $\text{AcO}^-$ ,  $\text{ClO}_4^-$ ,  $\text{BF}_4^-$ ,  $\text{PF}_6^-$  and  $\text{C}_6\text{H}_5\text{CO}_2^-$ . On the contrary, the presence of a  $\text{SO}_4^{2-}$  anion causes a dramatic increase of a structureless emission band at  $\lambda = 461$  nm and at  $\lambda = 472$  nm in the receptors 4 and 5, respectively, attributed to the formation of  $\pi$ -stacking interactions between two 1,4-naphthoquinone units<sup>22</sup> with a CHEF = 1068 for receptor 4 (see the ESI Fig. S30†) and 6894 for the halogenated receptor 5 (Fig. 4b). The presence of the  $\text{SO}_4^{2-}$

anion also causes an important increment of the quantum yield, 712 and 396 fold compared with the free receptors 4 and 5, respectively. Receptors 4 and 5 can be used as highly selective fluorescent “naked eye” chemosensors for the  $\text{SO}_4^{2-}$  anion due to the important increase of the fluorescence intensity in the visible region (Fig. 4a).

From the fluorescence titration, the detection limits for the  $\text{SO}_4^{2-}$  anion were  $1.34 \times 10^{-4}$  M for receptor 4 and  $1.39 \times 10^{-4}$  M for the halogenated receptor 5.

$^1\text{H-NMR}$  was used to obtain the structural information of the complexes formed by receptors 4 and 5 with  $\text{SO}_4^{2-}$  anions.

The  $^1\text{H NMR}$  spectra of receptor 4 in  $\text{CD}_3\text{CN}$  display the signals corresponding to the *meta* substituted phenyl moiety, used as the spacer at  $\delta$  ( $\text{H}_a$ ) = 8.88 ppm,  $\delta$  ( $\text{H}_b$ ) = 8.51 ppm and  $\delta$  ( $\text{H}_c$ ) = 7.88 ppm and the signals attributed to the naphthoquinone protons  $\text{H}_{c,d}$  and  $\text{H}_{g,f}$  at  $\delta = 8.13$  ppm and  $\delta = 7.89$  ppm, respectively. Interestingly, the olefinic quinone proton  $\text{H}_h$  appears downfield shifted at  $\delta = 7.04$  ppm with regards to that observed in the 2-hydroxy-1,4-naphthoquinone 1 ( $\delta = 6.25$  ppm) which could be attributed to the formation of intramolecular hydrogen bonding between the  $\text{H}_h$  proton with the oxygen of the carbonyl group of the ester. The halogenated receptor 5 shows a similar pattern of signals with the exception of the obvious absence of the proton  $\text{H}_h$ .

The stepwise addition of  $\text{SO}_4^{2-}$  anions to a solution of receptors 4 and 5 ( $c = 5 \times 10^{-3}$  M in  $\text{CD}_3\text{CN}/\text{MeOD}$  9:1) induced remarkable perturbations in the  $^1\text{H NMR}$  spectrum of the receptors. The observed perturbations are slow exchange processes wherein resonances corresponding to receptors 4 and 5 gradually disappear and resonances corresponding to new complexes appear during the titrations. The presence of the  $\text{SO}_4^{2-}$  anion in a solution of receptor 4 promotes only a small perturbation in the olefinic quinone proton  $\text{H}_h$  ( $\Delta\delta = -0.04$  ppm) which could be attributed to the simultaneous disruption of the intramolecular hydrogen bonding in receptor 4 and the formation of new hydrogen bonds between the  $\text{H}_h$  protons of the quinone and  $\text{SO}_4^{2-}$  anions. All the other protons were upfield shifted in both receptors. Taking into account the stoichiometry calculated by UV-Vis, these new resonances are assigned to the formation of a stable complex with a 2 : 1 receptor to anion stoichiometry. Additionally, practically all the resonances appear split indicating a low symmetry of the  $\text{SO}_4^{2-}$  complexes (Fig. 5 and S31†).

The association constants of the receptors 4 and 5 for the  $\text{SO}_4^{2-}$  anion in  $\text{CD}_3\text{CN}/\text{CD}_3\text{OD}$  by  $^1\text{HNMR}$  were calculated directly from the measurements of the concentrations of the free receptor and the complexes formed in solution by integration of the  $\text{H}_a$  resonances during the titration. The association constants of the receptors 4 and 5 for the  $\text{SO}_4^{2-}$  anion were  $K = 3.5 \times 10^4 \text{ mol}^{-2} \text{ L}^{-2}$  and  $K = 5.1 \times 10^4 \text{ mol}^{-2} \text{ L}^{-2}$  respectively.

As expected, in agreement with the data obtained previously from the UV-Vis spectroscopy, mass spectrometry and also the X-ray results,  $^1\text{H-NMR}$  titration experiments clearly indicate that the addition of  $\text{HP}_2\text{O}_7^{3-}$ ,  $\text{H}_2\text{PO}_4^-$ ,  $\text{F}^-$ ,  $\text{AcO}^-$  and  $\text{C}_6\text{H}_5\text{CO}_2^-$  to a solution of receptor 4 (in  $\text{CD}_3\text{CN}/\text{MeOD}$  9:1) and the

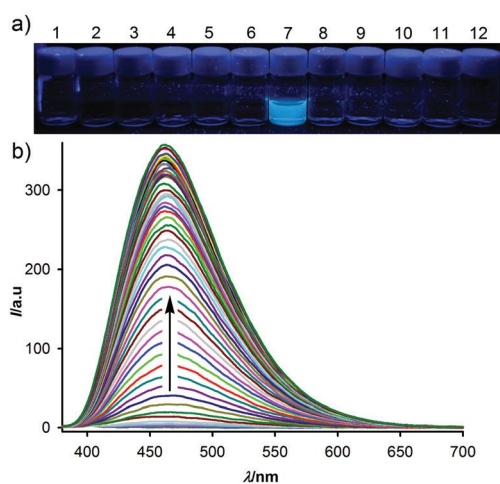


Fig. 4 (a) Visual changes in the fluorescence emission of receptor 4 (1) in  $\text{CH}_3\text{CN}$  upon the addition of  $\text{F}^-$  (2),  $\text{AcO}^-$  (3),  $\text{HP}_2\text{O}_7^{3-}$  (4),  $\text{C}_6\text{H}_5\text{CO}_2^-$  (5),  $\text{H}_2\text{PO}_4^-$  (6),  $\text{SO}_4^{2-}$  (7),  $\text{HSO}_4^-$  (8),  $\text{NO}_3^-$  (9),  $\text{Cl}^-$  (10),  $\text{Br}^-$  (11) and  $\text{I}^-$  (12). (b) Changes in the fluorescence spectra of receptor 4 ( $c = 5 \times 10^{-5}$  M in  $\text{CH}_3\text{CN}$ ) upon the addition of increasing amounts of  $\text{SO}_4^{2-}$  anions.

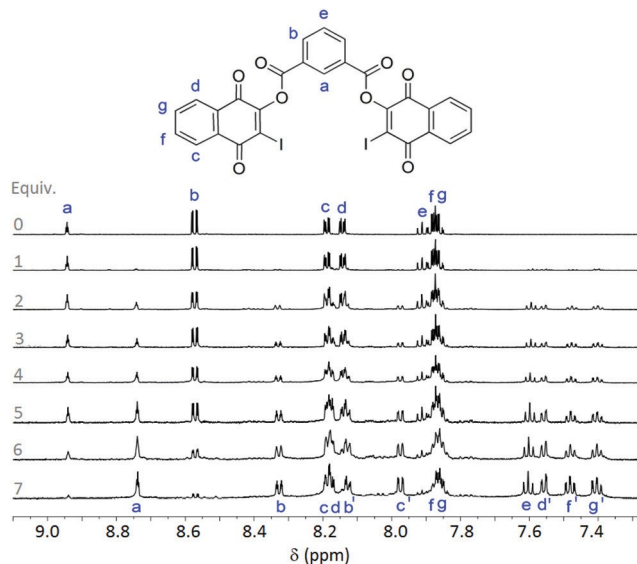


Fig. 5  $^1\text{H-NMR}$  spectral changes observed in receptor 5 in  $\text{CD}_3\text{CN}/\text{MeOD}$  9 : 1 during the addition of up to 7 equiv. of  $\text{SO}_4^{2-}$  anions.

addition of  $\text{HP}_2\text{O}_7^{3-}$ ,  $\text{F}^-$  and  $\text{AcO}^-$  to the halogenated receptor 5 (in  $\text{CD}_3\text{CN}/\text{MeOD}$  9 : 1) promotes the progressive disappearance of the receptor resonances and the appearance of new resonances corresponding to the rupture products of the receptors: 2-hydroxy-1,4-naphthoquinone or 3-iodo-2-hydroxy 1,4-naphthoquinone for receptors 4 or 5, respectively, and the signals corresponding to isophthalic acid (see the ESI Fig. S32–S39†).

#### Computational study

We have rationalized the binding mode of receptor 4 using DFT calculations (BP86-D3 functional and def2-TZVP basis set) and taking into consideration the solvent effects (acetonitrile).

We have first analysed the different conformers of receptors 4 and 5. For 4, we have found two isoenergetic conformers (difference within the accuracy of the theoretical method, *i.e.*,

$0.12 \text{ kcal mol}^{-1}$ ). The most energetically favoured conformation is represented in Fig. 6a. It is planar and presents two intramolecular H-bonding interactions involving the carbonylic O atom of the ester group and the H atom of the quinone ring. The other energetically stable conformation is not planar, Fig. 6b. For compound 5, the planar conformation is not stable due to the presence of the I atom instead of H, and the most stable conformers are represented in Fig. 6c.

In order to explore the parts of receptor 4 that are more suitable for interacting with anions, we have computed the molecular electrostatic potential (MEP) plotted onto the van der Waals surface in the most favored conformers (planar and non-planar, a and e). The MEP surface plots are shown in Fig. 7. It is interesting to note that in the planar conformer (intramolecular H-bond), two strong  $\pi$ -holes (the region of positive potential that is perpendicular to a portion of the molecular framework) are found, one over the carbonyl of the

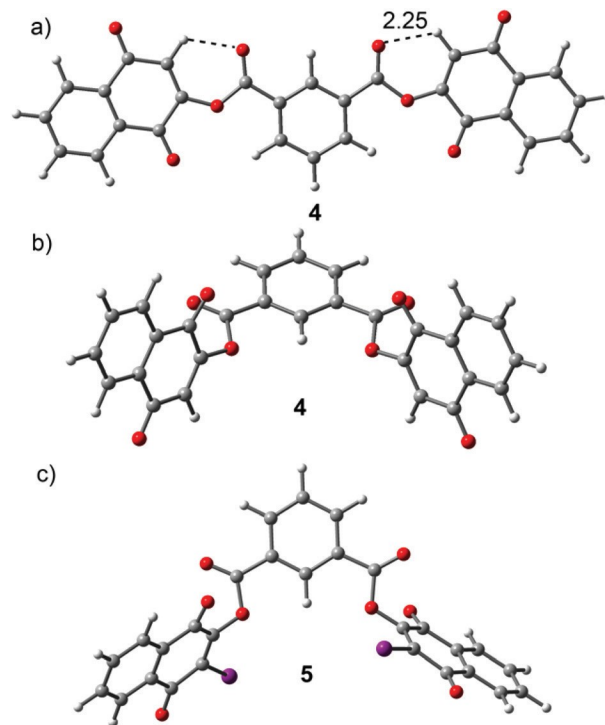


Fig. 6 Different conformers of receptors 4 (a) and (b) and 5 (c).

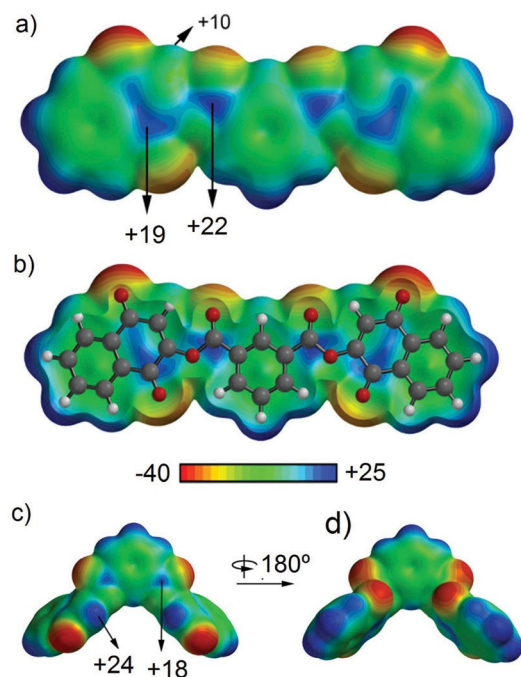


Fig. 7 MEP surfaces of two conformers of receptor 4. The energies in  $\text{kcal mol}^{-1}$  at selected points of the surfaces are given.

ester group ( $+22 \text{ kcal mol}^{-1}$ ) and the other over one C atom of the quinone ( $+19 \text{ kcal mol}^{-1}$ ). These  $\pi$ -holes are accessible from both sides of the molecular planes (see the open surface in Fig. 7b). The potential on the C–H bond of the quinone ring

( $\sigma$ -hole) is modest (+10 kcal mol<sup>-1</sup>) because it establishes the intramolecular H-bond. In sharp contrast, the nonplanar conformer (see Fig. 7c) shows the strongest potential value on the C–H bond of the quinone ring (+24). The  $\pi$ -hole is also observed over the ester group, however it is only accessible from one side of the ring (see Fig. 7d). This initial study reveals that the anion binding ability of this receptor is likely ruled by a delicate equilibrium between the interaction with the  $\pi$ -hole (carbon bonding interaction) and the formation of a C–H...X (X = anion) hydrogen bond with the concomitant weakening of the intramolecular C–H...O hydrogen bond.

This analysis strongly agrees with the fact that the most nucleophilic anions or the highly negatively charged HP<sub>2</sub>O<sub>7</sub><sup>3-</sup> are able to disrupt the ester group since the MEP value over the carbonyl group is large and positive due to the presence of the electron withdrawing quinone moiety.

All attempts to find noncovalent complexes between the anions and the planar conformation of the receptor failed because the optimization converges to the nucleophilic attack of the anion to the carbon atom of the ester carbonyl group.

We have also computed the host–guest complex of sulfate with receptors 4 and 5. The most convenient stoichiometry to trap the anion is 2 : 1 (receptor : anion) for both receptors. In the optimized geometry of the complex 4 with sulfate (see

Fig. 8a), it can be observed that each O atom of the sulfate participates in several H-bonding interactions involving the H atoms of the central phenyl ring of the receptor and the H-atom of the quinone moiety. Moreover, the complex also shows  $\pi$ -stacking interactions that are established between both receptors, thus contributing to the formation of the supramolecular assembly (Fig. 8). The interaction energy in acetonitrile is also indicated in the figure (–24.1 kcal mol<sup>-1</sup>).

The complex of sulfate with receptor 5 shows two equivalent halogen bonding interactions (I...O distance of 2.58 Å) and two anion– $\pi$  interactions with O...C distances ranging from 2.65 to 2.95 Å. It is worth mentioning that the interaction energy is more favorable for receptor 5 in qualitative agreement with the experimental results. It is also worth mentioning that the combination of halogen bonds and anion– $\pi$  interactions presents a higher ability to interact with sulfate than the C–H...O H-bonding network.

## Experimental

The reactions were performed using dried solvents and the solvents were previously dried by the traditional method. All melting points were determined by means of a Kofler hot-plate melting-point apparatus and are uncorrected. Solution NMR spectra were recorded on an NMR Bruker at 200, 300, 400, or 600 MHz. The abbreviations used in the NMR data are as follows: s (singlet), m (multiplet), and q (quaternary carbon atom). Tetramethylsilane (TMS) was used as an internal reference to determine the chemical shifts ( $\delta$ ) in the <sup>1</sup>H and <sup>13</sup>C NMR spectra. For the concentration used in the UV-Vis and fluorescence titration stated in the text and in the corresponding figure captions, we have used a 10 mm path length cell with the spectra background corrected before and after sequential additions of different aliquots of anions. The values of the quantum yield were calculated using anthracene as the standard ( $\Phi = 0.27 \pm 0.01$ ) and the following equation was derived  $\Phi_x/\Phi_s = (S_x/S_s) [(1-10^{-A_s})/(1-10^{-A_x})] (n^2/n_x^2)$ , where x and s indicate the unknown and standard solutions, respectively,  $\Phi$  is the quantum yield, S is the area under the emission curve, A is the absorbance at the excitation wavelength and n is the refractive index. The ESI-MS spectra were recorded on an Agilent 6300 LC/MS Ion Trap VL.

### Synthesis of bis(1,4-naphthoquinone-2-yl) isophthalate 4

Yield (200 mg, 84%). A solution of 2-hydroxy-1,4-naphthoquinone 1 (0.17 g, 1.0 mmol) in dichloromethane (10 mL) was treated with isophthaloyl dichloride 3 (0.10 g, 0.50 mmol) in the presence of 2,6-lutidine (0.23 mL, 2.0 mmol) at 0 °C and stirred for 20 min. The crude product was treated with 10% HCl. The organic layer was washed with water. The aqueous layer was extracted several times with dichloromethane. The combined organic layers were dried over anhydrous magnesium sulfate, filtered and dried *in vacuo* to give the product as a yellow pale solid: <sup>1</sup>H NMR (CDCl<sub>3</sub>, 400 MHz):  $\delta$ <sub>H</sub> 8.96 (1H, t, *J* = 1.8 Hz), 8.47 (2H, dd, *J* = 7.8 Hz, *J* = 1.8 Hz), 8.14–8.11

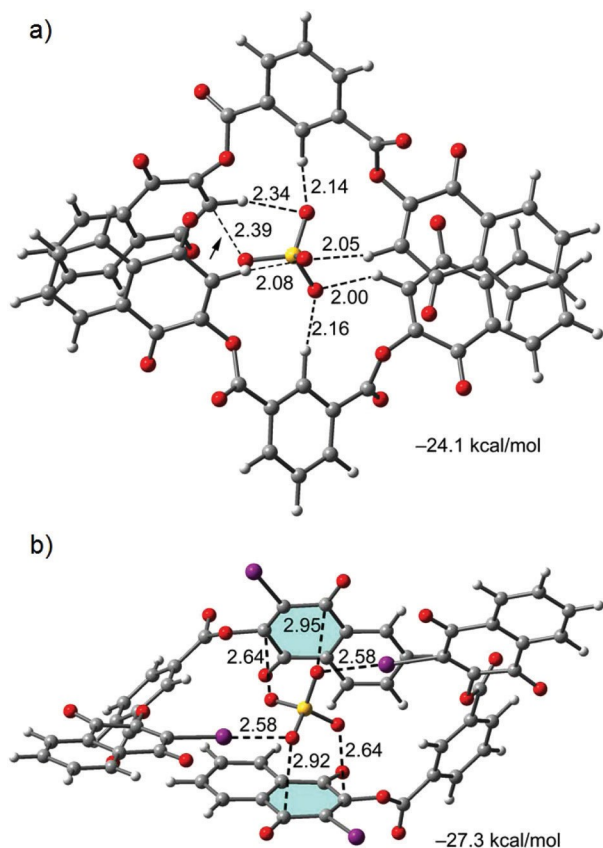


Fig. 8 Optimized complexes of sulfate with receptors 4 (a) and 5 (b). Distances are in Å. The noncovalent interactions are represented by the black dashed lines.

(4H, m), 7.80–7.76 (4H, m), 7.72 (1H, t,  $J = 7.8$  Hz), 6.94 (2H, s) ppm;  $^{13}\text{C}$  NMR (100 MHz,  $\text{CDCl}_3$ ):  $\delta_{\text{C}}$  185.37, 179.32, 163.50, 155.36, 137.00, 135.54, 135.13, 133.59, 132.89, 131.93, 130.54, 129.77, 128.04, 127.60, 127.38 ppm; MS (ESI):  $m/z$  calc. for  $[\text{M} + \text{H}]^+$  479.08, found 479.08; m.p = 208–209 °C.

#### Synthesis of bis(3-iodo-1,4-naphthoquinone-2-yl) isophthalate 5

Yield (240 mg, 67%). A solution of 3-iodo-2-hydroxy-1,4-naphthoquinone 2 (0.30 g, 1.0 mmol) in dichloromethane (10 mL) was treated with isophthaloyl dichloride 3 (0.10 g, 0.50 mmol) in the presence of 2,6-lutidine (0.23 mL, 2.0 mmol) at 0 °C and stirred for 20 min. The crude product was treated with 10% HCl. The organic layer was washed with water. The aqueous layer was extracted several times with dichloromethane. The combined organic layers were dried over anhydrous magnesium sulfate, filtered and dried *in vacuo*. The mixture was purified by column chromatography (elution with 1 : 1 hexane/EtOAc) to give the product as a yellow solid:  $^1\text{H}$  NMR ( $\text{CDCl}_3$ , 400 MHz):  $\delta_{\text{H}}$  9.05 (1H, t,  $J = 1.6$  Hz), 8.55 (2H, dd,  $J = 7.6$  Hz,  $J = 1.6$  Hz), 8.24–8.22 (2H, m), 7.18–8.16 (2H, m), 7.81–7.78 (5H, m) ppm;  $^{13}\text{C}$  NMR (100 MHz,  $\text{CDCl}_3$ ):  $\delta_{\text{C}}$  179.9, 175.68, 162.44, 159.83, 137.18, 135.55, 135.50, 133.89, 131.43, 131.40, 130.65, 129.77, 129.31, 128.54, 115.24 ppm; MS (ESI):  $m/z$  calc. for  $[\text{M} + \text{H}]^+$  729.86, found 729.86; m.p = 147–149 °C.

Crystal data for 3-iodo-1,4-1,4-dioxo-1,4-dihydronaphthalen-2-olate of tetrabutylammonium

$\text{C}_{26}\text{H}_{40}\text{INO}_3$ ,  $M = 541.49$ , monoclinic,  $a = 9.4286(5)$ ,  $b = 17.9956(10)$ ,  $c = 15.0794(7)$  Å,  $\beta = 92.7433(18)^\circ$ ,  $V = 2555.6(2)$  Å<sup>3</sup>, space group  $P2(1)/n$ ,  $Z = 4$ ,  $T = 120(2)$  K,  $\lambda = 0.71073$  Å,  $D_{\text{calcd}} = 1.407$  g cm<sup>-3</sup>,  $\mu = 1.279$  cm<sup>-1</sup>, 33 658 reflections were measured, 4854 unique ( $R_{\text{int}} = 0.867$ ) red crystals were obtained by Et<sub>2</sub>O/CH<sub>3</sub>CN vapour diffusion, the crystal structure solved by direct methods with all non hydrogen atoms refined anisotropically on  $F^2$  using the programs SHELXS-97 and SHELXL-2018,<sup>23</sup> the anion was disordered over two sites and was refined with 56(2)/44(2)% occupancies, the disordered anion moiety was refined with restrained bond lengths and angles and  $U_{ij}$  components (commands SAME, RIGU and ISOR), and hydrogen atoms were included using a riding model or as rigid methyl groups, GOF = 1.056,  $R(F_o, I > 2\sigma(I)) = 0.0577$ ,  $R_w(F^2, \text{all data}) = 0.1629$ .

CCDC 1915911† contains the supplementary crystallographic data for this paper.

#### Computational details

The energies of the conformations and complexes included in this study were computed at the B BP86-D3/def2-TZVP level of theory. The calculations have been performed by using the program TURBOMOLE version 7.0.<sup>24</sup> For the calculations, we have used the DFT-D functional with the latest available correction for dispersion (D3).<sup>25</sup> All structures were characterized by means of frequency analysis calculations at the BP86-D3/def2-TZVP level of theory. In order to reproduce the solvent

effects, we have used the conductor-like screening model COSMO,<sup>26</sup> which is a variant of the dielectric continuum solvation models.<sup>27</sup> We have used acetonitrile as the solvent.

## Conclusions

The results described herein provide evidence that 1,4-naphthoquinone and 3-iodo-1,4-naphthoquinone motifs can be used as anion binding sites. We have designed and synthesized two sulfate selective receptors based on these motifs that are able to recognize the anion by means of either a network of C–H⋯O bonds (4) or a combination of halogen bonds and anion– $\pi$  interactions (5), as demonstrated by DFT calculations. Finally, these motifs can be conveniently used to design novel anion receptors.

## Conflicts of interest

There are no conflicts to declare.

## Acknowledgements

This work was funded by the Ministerio de Economía y Competitividad of Spain and the FEDER ( projects CTQ2013-46096-P, CTQ2017-85821-R and CTQ2017-86775-P) and the Fundación Séneca Región de Murcia (CARM) ( projects 18948/JLI/13 and 20819/PI/18). We also thank Tobias Stuerzer at Bruker-Karlsruhe for the X-ray support and useful discussions.

## Notes and references

- (a) P. Molina, F. Zapata and A. Caballero, *Chem. Rev.*, 2017, 117, 9907–9972; (b) N. H. Evans and P. D. Beer, *Angew. Chem., Int. Ed.*, 2014, 53, 11716–11754; (c) P. A. Gale, N. Busschaert, C. J. E. Haynes, L. E. Karagiannidis and I. L. Kirby, *Chem. Soc. Rev.*, 2014, 43, 205–241; (d) L. E. Santos-Figueroa, M. E. Moragues, E. Climent, A. Agostini, R. Martínez-Mañez and F. Sancenon, *Chem. Soc. Rev.*, 2013, 42, 3489–3613; (e) P. A. Gale, E. N. W. Howe and X. Wu, *Chem*, 2016, 1, 351–422; (f) S. Kubik, *Chem. Soc. Rev.*, 2010, 39, 3648–3663.
- C. H. Park and H. E. Simmons, *J. Am. Chem. Soc.*, 1968, 90, 2431–2432.
- C. R. Bondy and S. J. Loeb, *Coord. Chem. Rev.*, 2003, 240, 77–99.
- V. Amendola, L. Fabbrizzi and L. Mosca, *Chem. Soc. Rev.*, 2010, 39, 3889–3915.
- J. L. Sessler, S. Camiolo and P. A. Gale, *Coord. Chem. Rev.*, 2003, 240, 17–55.
- (a) T. Romero, A. Caballero, A. Tarraga and P. Molina, *Org. Lett.*, 2009, 11, 3466–3469; (b) Q. Y. Cao, T. Pradhan, S. Kim and J. S. Kim, *Org. Lett.*, 2011, 13, 4386–4389; (c) P. Das, A. K. Mandal, M. K. Kesharwani, E. Suresh, B. Ganguly and

- A. Das, *Chem. Commun.*, 2011, 47, 7398–7400; (d) K. P. McDonald, Y. Hua, S. Lee and A. H. Flood, *Chem. Commun.*, 2012, 48, 5065–5075; (e) Y. Hua, R. O. Ramabhadran, J. A. Karty, K. Raghavachari and A. H. Flood, *Chem. Commun.*, 2011, 47, 5979–5981; (f) Y. Hua, R. O. Ramabhadran, E. O. Uduehi, J. A. Karty, K. Raghavachari and A. H. Flood, *Chem. – Eur. J.*, 2011, 17, 312–321; (g) B. Schulze and U. S. Schubert, *Chem. Soc. Rev.*, 2014, 43, 2522–2571 and references therein; (h) V. Haridas, S. Sahu, P. P. Kumar and A. R. Sapala, *RSC Adv.*, 2012, 2, 12594–12605; (i) M. Zurro and O. García Mancheño, *Chem. Rec.*, 2016, 17, 1–15.
- 7 (a) L. C. Gilday, N. G. White and P. D. Beer, *Dalton Trans.*, 2012, 41, 7092–7097; (b) Y. Hua, Y. Liu, C.-H. Chen and A. H. Flood, *J. Am. Chem. Soc.*, 2013, 135, 14401–14412; (c) J. Shang, W. Zhao, X. Li, Y. Wang and H. Jiang, *Chem. Commun.*, 2016, 52, 4505–4508; (d) S. Lee, B. E. Hirsch, Y. Liu, J. R. Dobscha, D. W. Burke, S. L. Tait and A. H. Flood, *Chem. – Eur. J.*, 2016, 22, 560–569; (e) J. Cai, B. P. Hay, N. J. Young, X. Yang and J. L. Sessler, *Chem. Sci.*, 2013, 4, 1560–1567; (f) D. Mungalpara, H. Kelm, A. Valkonen, K. Rissanen, S. Keller and S. Kubik, *Org. Biomol. Chem.*, 2017, 15, 102–113; (g) V. Martí-Centelles and P. D. Beer, *Chem. – Eur. J.*, 2015, 21, 9397–9404; (h) K. M. Mullen, J. Mercurio, C. J. Serpell and P. D. Beer, *Angew. Chem., Int. Ed.*, 2009, 48, 4781–4784.
- 8 (a) P. Sabater, F. Zapata, A. Caballero, I. Alkorta, C. Ramirez de Arellano, J. Elguero and P. Molina, *ChemistrySelect*, 2018, 3, 3855–3859; (b) F. Zapata, P. Sabater, A. Caballero and P. Molina, *Org. Biomol. Chem.*, 2015, 13, 1339–1346; (c) P. Sabater, F. Zapata, A. Caballero, N. de la Visitación, I. Alkorta, J. Elguero and P. Molina, *J. Org. Chem.*, 2016, 81, 7448–7458; (d) J. Y. Kwon, N. J. Singh, H. Kim, S. K. Kim, K. S. Kim and J. Yoon, *J. Am. Chem. Soc.*, 2004, 126, 8892–8893; (e) Y. Bai, B.-G. Zhang, J. Xu, C.-Y. Duan, D.-B. Dang, D.-J. Liu and Q.-J. Meng, *New J. Chem.*, 2005, 29, 777–779; (f) V. Amendola, M. Boiocchi, B. Colasson, L. Fabbrizzi, E. Monzani, M. J. Douton-Rodriguez and C. Spadini, *Inorg. Chem.*, 2008, 47, 4808–4816; (g) Z. Xu, N. J. Singh, J. Lim, J. Pan, H. N. Kim, S. Park, K. S. Kim and J. Yoon, *J. Am. Chem. Soc.*, 2009, 131, 15528–15533; (h) Ch. E. Willans, K. M. Anderson, L. C. Potts and J. W. Steed, *Org. Biomol. Chem.*, 2009, 7, 2756–2760; (i) D. P. Cormode, S. S. Murray, A. R. Cowley and P. D. Beer, *Dalton Trans.*, 2006, 5135–5140; (j) K. Chellappan, N. J. Singh, I.-C. Hwang, J. W. Lee and K. S. Kim, *Angew. Chem., Int. Ed.*, 2005, 44, 2899–2903; (k) L. Yang, S. Qin, X. Su, F. Yang, J. You, Ch. Hu, R. Xie and J. Lan, *Org. Biomol. Chem.*, 2010, 8, 339–348; (l) H.-T. Niu, Z. Yin, D. Su, D. Niu, J. He and J.-P. Cheng, *Dalton Trans.*, 2008, 3694–3700.
- 9 (a) G. Cavallo, P. Metrangolo, R. Milani, T. Pilati, A. Primagi, G. Resnati and G. Terraneo, *Chem. Rev.*, 2016, 116, 2478–2601; (b) L. C. Gilday, S. W. Robinson, T. A. Barendt, M. J. Langton, B. R. Mullaney and P. D. Beer, *Chem. Rev.*, 2015, 115, 7118–7195.
- 10 P. Metrangolo, F. Meyer, T. Pilati, G. Resnati and G. Terraneo, *Angew. Chem., Int. Ed.*, 2008, 47, 6114–6127.
- 11 P. Politzer, J. S. Murray and T. Clark, *Phys. Chem. Chem. Phys.*, 2010, 12, 7748–7757.
- 12 (a) F. Zapata, A. Caballero, P. Molina, I. Alkorta and J. Elguero, *J. Org. Chem.*, 2014, 79, 6959–6969; (b) N. L. Kilah, M. D. Wise, C. J. Serpell, A. L. Thompson, N. G. White, K. E. Christensen and P. D. Beer, *J. Am. Chem. Soc.*, 2010, 132, 11893–11895; (c) J. M. Mercurio, R. C. Knighton, J. Cookson and P. D. Beer, *Chem. – Eur. J.*, 2014, 20, 11740–11749; (d) B. R. Mullaney, A. L. Thompson and P. D. Beer, *Angew. Chem., Int. Ed.*, 2014, 53, 11458–11462; (e) L. González, F. Zapata, A. Caballero, P. Molina, C. Ramírez de Arellano, I. Alkorta and J. Elguero, *Chem. – Eur. J.*, 2016, 22, 7533–7544.
- 13 (a) F. Zapata, S. J. Benítez-Benítez, P. Sabater, A. Caballero and P. Molina, *Molecules*, 2017, 22, 2273; (b) C. J. Serpell, N. L. Kilah, P. J. Costa, V. Félix and P. D. Beer, *Angew. Chem., Int. Ed.*, 2010, 49, 5322–5326; (c) A. Caballero, F. Zapata, N. G. White, P. J. Costa, V. Félix and P. D. Beer, *Angew. Chem., Int. Ed.*, 2012, 51, 1876–1880; (d) A. Caballero, N. G. White and P. D. Beer, *Angew. Chem., Int. Ed.*, 2011, 50, 1845–1848; (e) F. Zapata, A. Caballero, N. G. White, T. D. W. Claridge, P. J. Costa, V. Félix and P. D. Beer, *J. Am. Chem. Soc.*, 2012, 134, 11533–11541; (f) M. Cametti, K. Raatikainen, P. Metrangolo, T. Pilati, G. Terraneo and G. Resnati, *Org. Biomol. Chem.*, 2012, 10, 1329–1333; (g) P. Sabater, F. Zapata, A. Caballero, N. de la Visitación, I. Alkorta, J. Elguero and P. Molina, *J. Org. Chem.*, 2016, 81, 7448–7458.
- 14 L. C. Gilday, T. Lang, A. Caballero, P. J. Costa, V. Félix and P. D. Beer, *Angew. Chem., Int. Ed.*, 2013, 52, 4356–4360.
- 15 (a) A. Mele, P. Metrangolo, H. Neukirch, T. Pilati and G. Resnati, *J. Am. Chem. Soc.*, 2005, 127, 14972–14973; (b) M. G. Sarwar, B. Dragisic, S. Sagoo and M. S. Taylor, *Angew. Chem., Int. Ed.*, 2010, 49, 1674–1677; (c) M. G. Chudzinski, C. A. McClary and M. S. Taylor, *J. Am. Chem. Soc.*, 2011, 133, 10559–10567.
- 16 (a) F. Zapata, A. Caballero and P. Molina, *Eur. J. Inorg. Chem.*, 2017, 237–241; (b) L. C. Gilday, N. G. White and P. D. Beer, *Dalton Trans.*, 2013, 42, 15766–15773; (c) M. J. Langton, S. W. Robinson, I. Marques, V. Félix and P. D. Beer, *Nat. Chem.*, 2014, 6, 1039–1043.
- 17 R. Saini, N. Kaur and S. Kumar, *Tetrahedron*, 2014, 70, 4285–4307.
- 18 E. Hatzigrigoriou, S. Spyroudis and A. Varvoglis, *Liebigs Ann. Chem.*, 1989, 167–170.
- 19 S. B. Zaware, S. Dagade-Waghmode, R. G. Gonnade, D. Srinivas and S. Y. Rane, *J. Mol. Struct.*, 2009, 938, 328–335.
- 20 P. Rodriguez-Cuamatzi, O. I. Arillo-Flores, M. I. Bernal-Uruchurtu and H. Hoepfl, *Supramol. Chem.*, 2007, 19, 559–578.



- 21 P. Kuzmic, *Anal. Biochem.*, 1996, 237, 260–273.
- 22 B. R. Jali and J. B. Baruah, *Dyes Pigm.*, 2014, 110, 56–66.
- 23 G. M. Sheldrick, *Acta Crystallogr., Sect. C: Struct. Chem.*, 2015, 71, 3–8.
- 24 R. Ahlrichs, M. Bär, M. Hacer, H. Horn and C. Kömel, *Chem. Phys. Lett.*, 1989, 162, 165–169.
- 25 S. Grimme, J. Antony, S. Ehrlich and H. Krieg, *J. Chem. Phys.*, 2010, 132, 154104–154119.
- 26 A. Klamt and G. Schüürmann, *J. Chem. Soc., Perkin Trans. 2*, 1993, 799–805.
- 27 A. Klampt, *Wiley Interdiscip. Rev.: Comput. Mol. Sci.*, 2011, 1, 699–709.